Crosshole seismic tomography: working solutions to issues in real data travel time inversion

2005 J. Geophys. Eng. 2 139

(http://iopscience.iop.org/1742-2140/2/2/008)

Nanjing Institute of Geophysical Prospecting and Institute of Physics Publishing — Journal of Geophysics and Engineering

J. Geophys. Eng. **2** (2005) 139–146 doi:10.1088/1742-2132/2/2/008

Crosshole seismic tomography: working solutions to issues in real data travel time inversion

Ying Rao and Yanghua Wang

Centre for Reservoir Geophysics, Department of Earth Science and Engineering,
Imperial College London, South Kensington, London SW7 2BP, UK

E-mail: yanghua.wang@imperial.ac.uk

Received 14 December 2004
Accepted for publication 26 April 2005
Published 20 May 2005
Online at stacks.iop.org/JGE/2/139

Abstract
In travel time inversion of crosshole seismic tomography, when dealing with real data, the following three issues need to be addressed: how to suppress the effect of data errors, how to balance the data contribution and reference model, and how to properly set the geological constraints (well logs) in an inversion. Signal-to-noise ratios of travel time data picked from real crosshole seismic surveys likely depend on the vertical offset between a source and a receiver, since the overall attenuation will typically be greater for a longer ray path. Therefore, to suppress the effect of data errors in a least-squares solution, a data confidence matrix is used in practice where the weighting is set logically based on the vertical offset. When a model constraint is adopted in the inversion to seek a solution with least deviation from some prescribed background that is most likely to have no spurious structure, a trade-off parameter is used to explicitly balance the dependence of the inversion solution to the data contribution and the reference model. The latter is built by combining sonic logging information, which is hard geological evidence at the vicinity of wells, and an initial estimate from the travel time back-projection, a preliminary solution of the travel time tomography. Geological constraints are set so that the inversion solution should have the least deviation from the hard geological evidence, and more deviation for the remaining part of the survey region, since the true velocity model might differ from such an initial estimate and the true ray paths might deviate from the initial ray paths.

Keywords: seismic tomography, travel time inversion, inverse problem, inversion constraints, crosshole seismic

1. Introduction

Seismic travel time inversion for velocity structure is a nonlinear problem since seismic rays, acting as the integral paths in a tomographic inversion, depend also on the medium velocity (Worthington 1984, Zhou and Greenhalgh 2003). Instead of determining the unknown ray paths and the unknown velocity structure simultaneously, one often uses a linearized solution iteratively to solve for the model perturbations rather than the model parameters directly (Bording *et al* 1987). Model perturbations are assumed to be small enough so that one can then consider the relationship between the model perturbations and the corresponding residuals as linear. Once the model perturbations have been found, they are added to the current model to produce the model for the following iteration until the result converges.

In practice, seismic data sometimes contain a considerable amount of noise. For travel time data, finite reading accuracy is a main source of data errors. To reduce the errors, one pre-processing method is to average the travel time data from similar ray paths (Röhm *et al* 2000), but this method may only work on teleseimic tomography as the errors are relatively small compared to the actual travel time data. To mitigate the data errors, Wang *et al* (2000) winnowed the noisy travel time data using a locally weighted regression to get rid of the outliers or down-weight the large picking errors. To reduce the effect of data errors during the inversion, Scales *et al* (1988) used weighting coefficients as a function of the travel time residual in an iteratively reweighted least-squares scheme. Such residual-based weights however are subjective, since the data errors in practice might have a non-Gaussian distribution and thence the data residual might be biased. Cao and Greenhalgh (1995) gave a relative error-based nonlinear inversion scheme for crosshole seismic data which attempts to overcome the bias of least-squares methods which tend to emphasize rays with greater travel times. In this paper, we attempt to tackle this head-on as follows through a data confidence matrix. Observations from real seismic data between two parallel vertical wells, as shown in this paper, indicate that the signal-to-noise ratios likely depend on the vertical offset between a source and a receiver. It follows logically that we should set the weight inversely based on the vertical offset, a reflection of our confidence in the accuracy of the picked travel time. This idea is similar to Berryman's (1989) scheme, in which a smaller weight was given to the longer ray paths that are affected by many different pixel slownesses (inverse velocities).

The seismic inversion problem is ill-conditioned and ill-posed so there may be no exact solution (Groetsch 1993). Sources and receivers can rarely be placed on all sides of the region to be imaged, resulting in some sub-regions having very poor ray coverage. Under such circumstances, one practical solution is obtained by applying additional constraints to the inverse problem, e.g., upper and lower limits to the reconstructed velocities (van Wijk *et al* 2002). This involves searching for a solution that not only satisfies the data but also is 'close', in some adjustable sense, to some initial model that must be specified. In this paper, sonic logging data sets are used to define such an initial model.

This paper is organized as follows. We start with a simple derivation from a nonlinear inversion objective function to a linearized inverse equation, so as to recap the physical meaning of the following three parameters in an inverse problem: (a) a data covariance matrix, denoted $\mathbf{C}_\mathrm{D}$, (b) a trade-off parameter μ and (c) a model covariance matrix denoted $\mathbf{C}_\mathrm{M}$. Keeping their physical meaning in mind, we then attempt to offer a working definition to each of these three parameters, which are sometimes mathematically tedious in inverse theory.

2. The linear inverse problem

The least-squares inverse problem is to infer a model that minimizes the difference between the theoretical prediction and the observed data set, and meanwhile, is close to a reference model. The objective function is given as (Tarantola 2005)

$$J(\mathbf{m}) = [f(\mathbf{m}) - \mathbf{d}]^\mathrm{T}\,\mathbf{C}_\mathrm{D}^{-1}[f(\mathbf{m}) - \mathbf{d}] + \mu(\mathbf{m} - \mathbf{m}_0)^\mathrm{T}\,\mathbf{C}_\mathrm{M}^{-1}(\mathbf{m} - \mathbf{m}_0), \qquad (1)$$

where $\mathbf{m}$ is the current model vector, $f(\mathbf{m})$ is the forward prediction for the current model, $\mathbf{d}$ is the vector of the observed data set, $\mathbf{C}_\mathrm{D}$ is called the data covariance matrix with physical units of (data)^2, $\mathbf{m}_0$ is a reference model, $\mathbf{C}_\mathrm{M}$ is called the model covariance matrix with units of (model parameter)^2, and the scalar μ is a trade-off parameter that controls the relative weights of the data contribution and the reference information. In this paper, the velocity model between two vertical wells is parametrized as regular cells and model $\mathbf{m}$ is the N-vector whose element m_j is the slowness (inverse velocity) in the jth cell. Other possible choices of parametrizations are Fourier expansion (Wang and Houseman 1995), B-splines and polynomial expansion, etc (Spakman and Bijwaard 2001, Rawlinson and Sambridge 2003). The data vector $\mathbf{d}$ consists of M travel time picks.

To solve this minimization problem, we set $\partial J/\partial m_j = 0$, for $j = 1, 2, \ldots, N$, and obtain

$$\mathbf{G}^\mathrm{T}\mathbf{C}_\mathrm{D}^{-1}[f(\mathbf{m}) - \mathbf{d}] + \mu\mathbf{C}_\mathrm{M}^{-1}(\mathbf{m} - \mathbf{m}_0) = 0, \qquad (2)$$

where $\mathbf{G} = \nabla_\mathbf{m} f(\mathbf{m})$ is the matrix of the Fréchet derivatives of the forward modelling $f(\mathbf{m})$ with respect to the model parameters $\mathbf{m}$. For ray-based travel time modelling,

$$f(\mathbf{m}) = \mathbf{A}\mathbf{m}, \qquad (3)$$

where $\mathbf{A}$ is the $M \times N$ matrix with element a_{ij} denoting the ray length of the ith ray in the jth cell of a subdivision of the model space. Curvilinear ray trajectories are traced through the current model $\mathbf{m}$ using Fermat's principle (Wang and Houseman 1995, Wang 2003). Substituting (3) into (2), we have

$$\mathbf{A}^\mathrm{T}\mathbf{C}_\mathrm{D}^{-1}[\mathbf{A}\mathbf{m} - \mathbf{d}] + \mu\mathbf{C}_\mathrm{M}^{-1}(\mathbf{m} - \mathbf{m}_0) = 0. \qquad (4)$$

As the ray path that constitutes matrix $\mathbf{A}$ in equation (3) is also model $\mathbf{m}$ dependent, travel time inversion (4) is a nonlinear problem. Given a perturbation to the model, i.e. $\mathbf{m} = \mathbf{m}_0 + \delta\mathbf{m}$, equation (4) becomes

$$\left(\mathbf{A}^\mathrm{T}\mathbf{C}_\mathrm{D}^{-1}\mathbf{A} + \mu\mathbf{C}_\mathrm{M}^{-1}\right)\delta\mathbf{m} = \mathbf{A}^\mathrm{T}\mathbf{C}_\mathrm{D}^{-1}[\mathbf{d} - \mathbf{A}\mathbf{m}_0], \qquad (5)$$

where $\delta\mathbf{m}$ is the vector of model perturbation (slowness updating). The explicit solution to the linear system (5) is

$$\delta\mathbf{m} = \left(\mathbf{A}^\mathrm{T}\mathbf{C}_\mathrm{D}^{-1}\mathbf{A} + \mu\mathbf{C}_\mathrm{M}^{-1}\right)^{-1}\mathbf{A}^\mathrm{T}\mathbf{C}_\mathrm{D}^{-1}\delta\mathbf{d}, \qquad (6)$$

where $\delta\mathbf{d} \equiv \mathbf{d} - \mathbf{A}\mathbf{m}_0$ is the vector of the data residuals (relative to the reference model). We solve this linear equation using a conjugate gradient method (Hanke 1995, Engl *et al* 1996).

The simple derivation summarized in this section clearly shows that three parameters, $\mathbf{C}_\mathrm{D}^{-1}$, μ and $\mathbf{C}_\mathrm{M}^{-1}$, in the linear equation (6) are from the nonlinear inversion objective function (1). Thus, each of these three parameters in the linear equation (6) has an explicit physical meaning: (a) $\mathbf{C}_\mathrm{D}^{-1}$ is the inverse data covariance matrix, (b) μ is the trade-off parameter and (c) $\mathbf{C}_\mathrm{M}^{-1}$ is the inverse model covariance matrix. In the following three sections, we attempt to provide a working definition for each of them, associated with real data applications of crosshole travel time tomography.

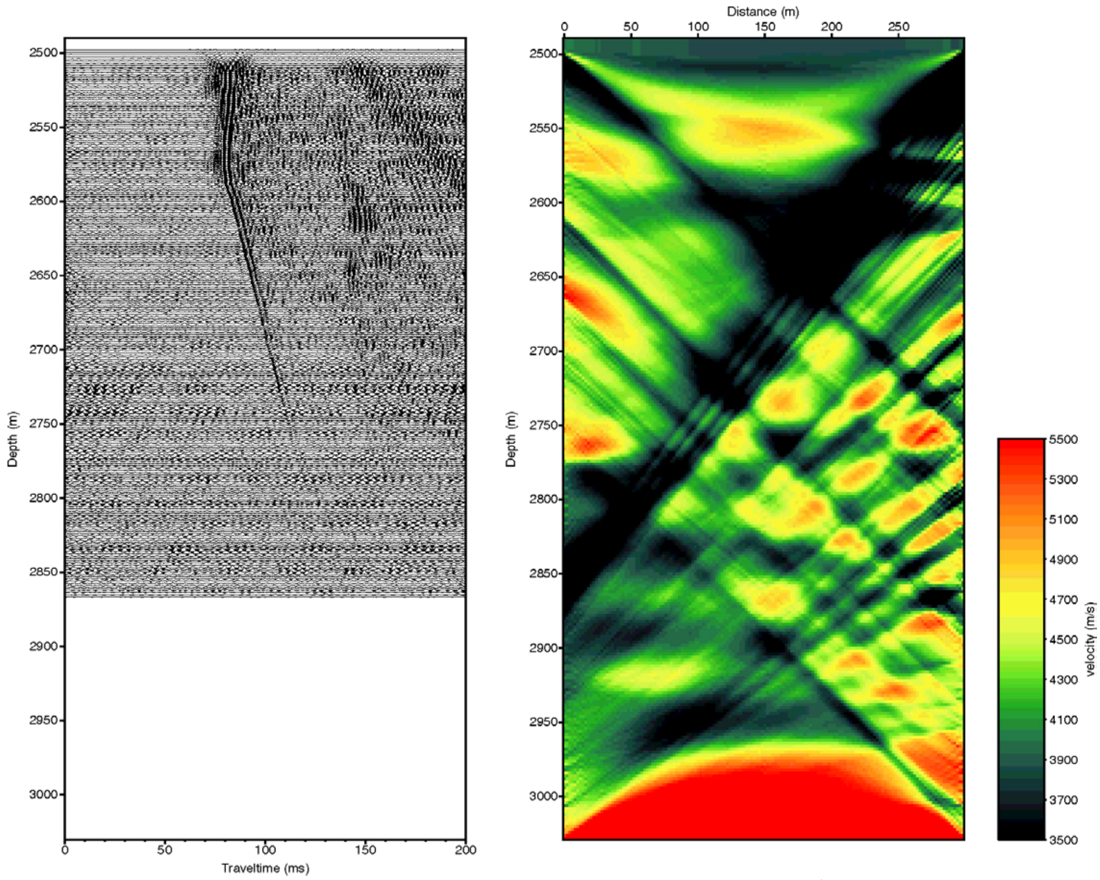

(*a*) (*b*)

Figure 1. (*a*) A sample shot gather of a crosshole seismic showing the uncertainty of the first arrivals in the far offset traces. (*b*) The preliminary result of travel time inversion showing strong artefacts due to travel time picking errors.

3. Suppressing the effect of data errors

In this section, we attempt to suppress the effect of data errors in the least-squares problem by defining a so-called confidence matrix pragmatically, i.e. a working solution for $\mathbf{C}_\mathrm{D}^{-1}$, the inverse of data covariance matrix.

When seeking a model $\mathbf{m}$ that minimizes the difference between the theoretical prediction $f(\mathbf{m})$ and the observation $\mathbf{d}$ in a least-squares sense, the objective function is given as

$$J(\mathbf{m}) = [f(\mathbf{m}) - \mathbf{d}]^\mathrm{T}\mathbf{C}_D^{-1}[f(\mathbf{m}) - \mathbf{d}], \tag{7}$$

which is the first term only of expression (1). The linear solution can be written as

$$\delta\mathbf{m} = \left(\mathbf{A}^\mathrm{T}\mathbf{C}_\mathrm{D}^{-1}\mathbf{A}\right)^{-1}\mathbf{A}^\mathrm{T}\mathbf{C}_\mathrm{D}^{-1}\delta\mathbf{d}. \tag{8}$$

The observed data $\mathbf{d}$, which in this study are first arrival times, inevitably contain errors of many different forms, such as noise disturbance, instrument errors and travel time picking errors. Their actual values remain indeterminate, but if errors can be treated as random variables, their statistical properties, such as the expected value, variances and covariance, can be estimated. In the least-squares formula (7), errors are implicitly treated as random variables. This is what the data covariance matrix $\mathbf{C}_\mathrm{D}$ is usually referred to.

For teleseismic tomography, mispicks of onsets or incorrect phase association can be treated as random errors that may not yield any significant bias to the tomographic model parameters, because these errors are so small compared to the travel time measurement (Röhm *et al* 2000). In crosshole seismic tomography, however, these data-picking errors may not be treated as random variables with a Gaussian distribution and the solution may often be biased. Figure 1(*a*) is a sample shot gather on which the first arrivals of the far offset traces cannot be clearly identified and thus the picked times are not reliable at all. If those travel times were used in the inversion, the resultant image would have strong artefacts as shown in figure 1(*b*).

In this paper, we attempt to combat these erroneous travel times in the inverse problem by properly setting the matrix $\mathbf{C}_\mathrm{D}^{-1}$ in the least-squares formula (7). Matrix $\mathbf{C}_\mathrm{D}^{-1}$ here is no longer an explicit statistical measurement of the data errors. Instead, we define it pragmatically as a diagonal matrix with positive definitive elements, representing our confidence in each individual travel time pick, as

$$\mathbf{C}_\mathrm{D}^{-1} = \mathrm{diag}\{c_i\}, \tag{9}$$

where c_i is the estimated certainty of the ith measurement and, in this case, cross correlation between data errors is ignored.

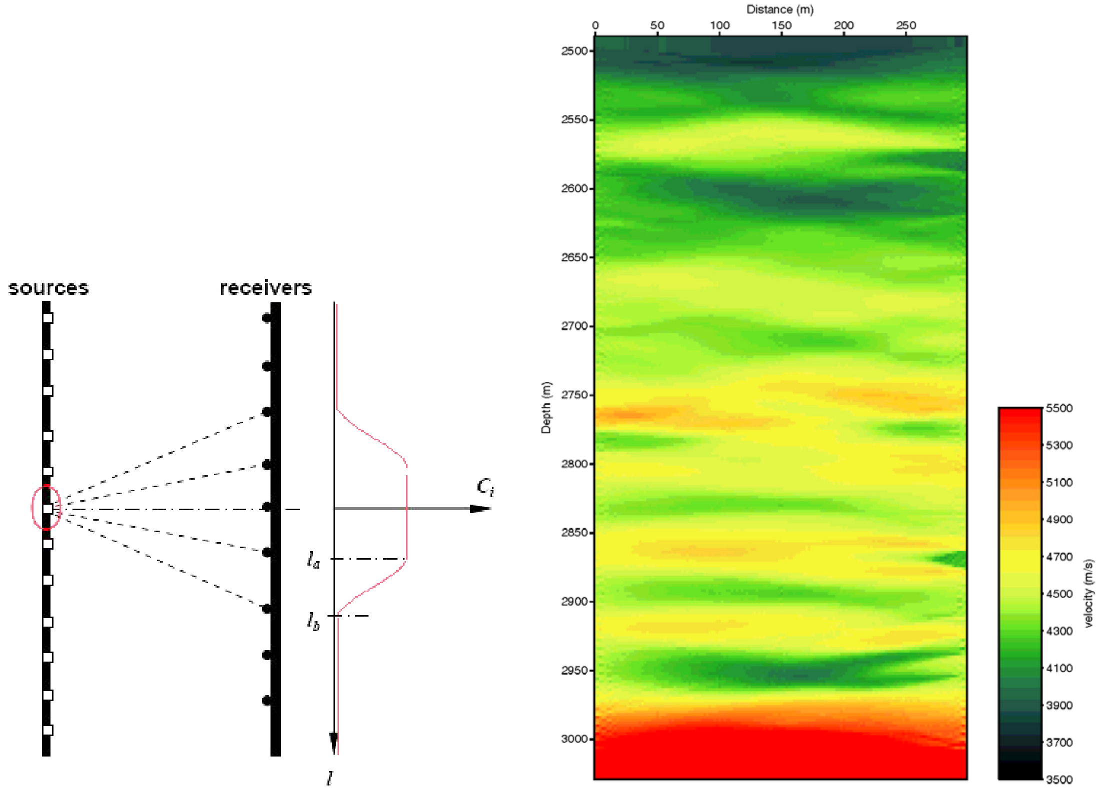

(*a*) (*b*)

Figure 2. (*a*) The data certainty, c_i, of the *i*th travel time pick is defined in terms of the (normalized) vertical offset *l*, and is used to build the data confidence matrix, which is conventionally referred to as the inverse of the data covariance matrix. (*b*) The inversion result suggests that the data-error effect has been suppressed successfully, by using the data confidence matrix.

For the ray between the *i*th source–receiver pair, as shown schematically in figure 2(*a*), the data certainty is defined in terms of the vertical offset as

$$c_i = \begin{cases} 1, & \text{for} \quad \ell \leqslant \ell_a, \\ 0.51 + 0.49\cos\left(\dfrac{\ell - \ell_a}{\ell_b - \ell_a}\pi\right), & \text{for} \quad \ell_a < \ell \leqslant \ell_b, \\ 0.02, & \text{for} \quad \ell \geqslant \ell_b, \end{cases} \tag{10}$$

where ℓ is the normalized vertical offset $\ell = |z_r - z_s|/|x_r - x_s|$ between a source at (x_s, z_s) and a receiver at (x_r, z_r). The smaller the vertical offset is, the more certain the observation should be, since the overall attenuation will typically be smaller for a shorter ray path and hence the sharpness and strength of arrival increases. Another argument given for such weights is that the ray paths with small vertical offset are more likely to correspond to real ray paths that remain completely in the image plane for two-dimensional reconstruction problems. In fact, this was the motivation for Berryman's (1989) weighting scheme in which rays of greatest length were weighted least in the reconstruction.

The choice of parameters ℓ_a and ℓ_b in expression (10) can be somewhat arbitrary. We set them here based on a limited number of experiments, in which ℓ_a is more or less fixed but ℓ_b is the parameter that is adjusted according to the inversion result. For the rest of this paper, the images shown are obtained with $\ell_a = 0.2$ and $\ell_b = 0.5$. By using this working solution, we produce an encouraging result as shown in figure 2(*b*) in which the layered structure, indicated by the reflection image of the crosshole seismic data (not shown here), has been reconstructed and some velocity anomalies have been shown clearly. For this real data example, the actual survey area is $X = 300$ m and $Z = 540$ m. In the ray-based tomographic inversion, we divide it into 150×270 grid points with cell size of 2 m.

4. Balancing the contribution of data minimization and *a priori* model

The inversion process needs to achieve a balance between what is mathematically possible and geological reality. The balance is dependent on the approach taken in setting up the inversion problem, the choice of criteria to optimize and establishing what constitutes 'optimal' for that problem. In this section, we attempt to somehow quantitatively balance the contribution from the data minimization and from the *a priori* model, by testing the trade-off parameter, μ.

Given an *a priori* model $\mathbf{m}_0$, the objective function is given as expression (1), and the linear solution is written as equation (6), in which parameter μ acts as a dimensionless damping factor, introduced to stabilize the inverse procedure. In this section where we are testing the parameter μ, we simply

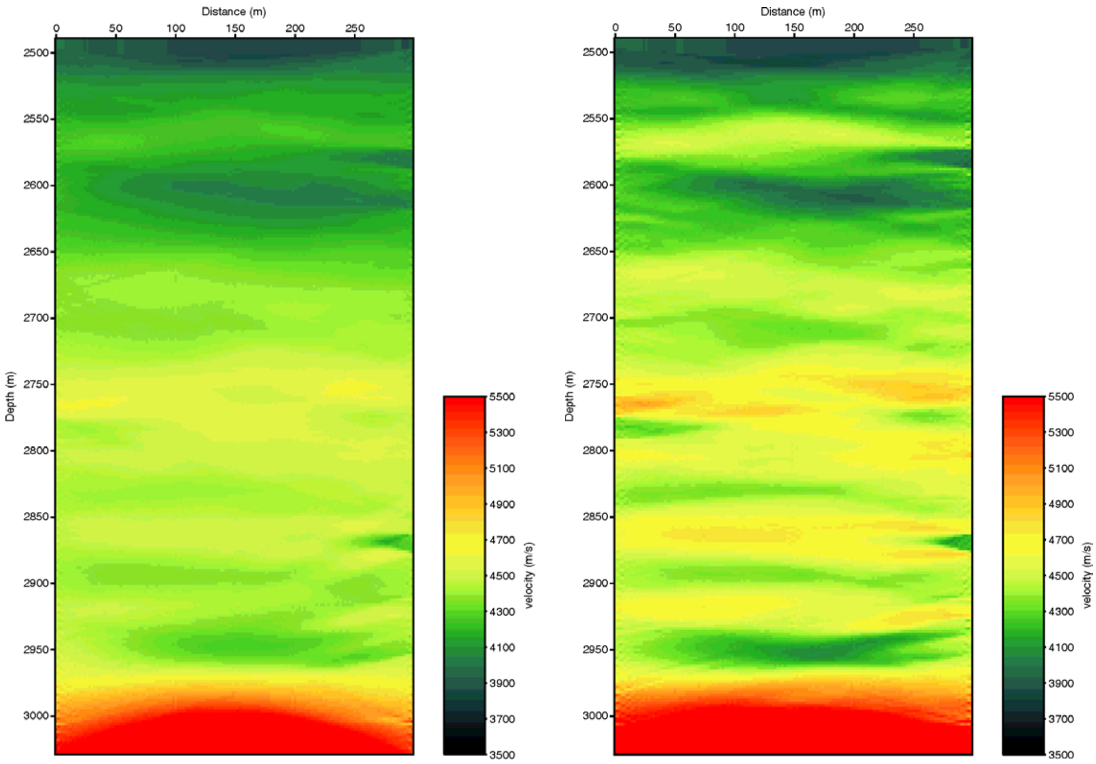

(*a*) (*b*)

Figure 3. (*a*) The *a priori* model, and (*b*) the tomographic image using $\mu = 0.3$.

set $\mathbf{C}_\mathrm{M}^{-1} = \kappa\mathbf{I}$, where $\mathbf{I}$ is the dimensionless identity matrix, κ is a normalizing factor with units of (model parameter)$^{-2}$ given by (Wang and Pratt 1997)

$$\kappa = \frac{\mathrm{trace}\left(\mathbf{A}^\mathrm{T}\mathbf{C}_\mathrm{D}^{-1}\mathbf{A}\right)}{n_r}, \tag{11}$$

and n_r is the total number of ray paths. After the use of the normalizing factor κ, parameter μ is then chosen within the interval [0, 1].

Various assumptions are incorporated in any inversion procedure and there are non-uniqueness bounds on the inverted model. The motivation for using the model constraint term in the objective function (1) is that, although there may be many solutions to the inverse problem, the ones with least deviation from some intelligently prescribed background, $\mathbf{m}_0$, are most likely to have no spurious structure. The trade-off parameter μ then controls the dependence of the final inversion result on the initial *a priori* model. In this test the *a priori* model as shown in figure 3(*a*) is built from travel time back-projection (Worthington 1984) with the data certainty matrix $\mathbf{C}_\mathrm{D}^{-1}$ described above to suppress the effect of travel time picking errors. Figure 3(*b*) is the tomographic image using an example value of $\mu = 0.3$.

We have tested different μ values. When μ increases, the resulting velocity model is more and more similar to the *a priori* model. The top and bottom parts are more similar to the elliptic character of the *a priori* model; the 2600–2750 m depth portion is more similar to the cloudy character of the reference model. From the convergence rates, as shown in figure 4, we can see that when $\mu = 0.1$, the inversion has a steady convergence, even after 16 iterations. There is a potential risk of misinterpreting spurious noise in the data as a geological feature. When $\mu = 0.3$, 0.5 and 0.7, the inversions show clear dependence on the *a priori* model. For $\mu = 0.7$ the convergence rate decreases after four iterations. For $\mu = 0.5$ the convergence rate decreases after six iterations. For $\mu = 0.3$ the convergence rate decreases after eight iterations. Therefore, in the rest of the tests, we choose $\mu = 0.3$ and the image of the eighth iteration as the final result.

5. Well-log constraint in the inversion

The inverse problem in geophysics is generally under-determined, which necessitates the introduction of additional constraints on the model parameters in order to obtain a unique solution. In using sonic logging information as a geological constraint in the inverse problem, we discuss two schemes in this section.

In the first scheme, we construct an initial model by combining the logging velocity and the velocity field obtained from the travel time back-projection. In the initial model, the velocity within the kth cell in the x direction, $v_k^{(\mathrm{init})}$, is given by

$$v_k^{(\mathrm{init})} = \omega_k v_k^{(\mathrm{log})} + (1 - \omega_k) v_k^{(\mathrm{t})}, \tag{12}$$

where $v_k^{(\mathrm{log})}$ is the logging velocity, $v_k^{(\mathrm{t})}$ is the velocity obtained from travel time back projection and ω_k is a weighting

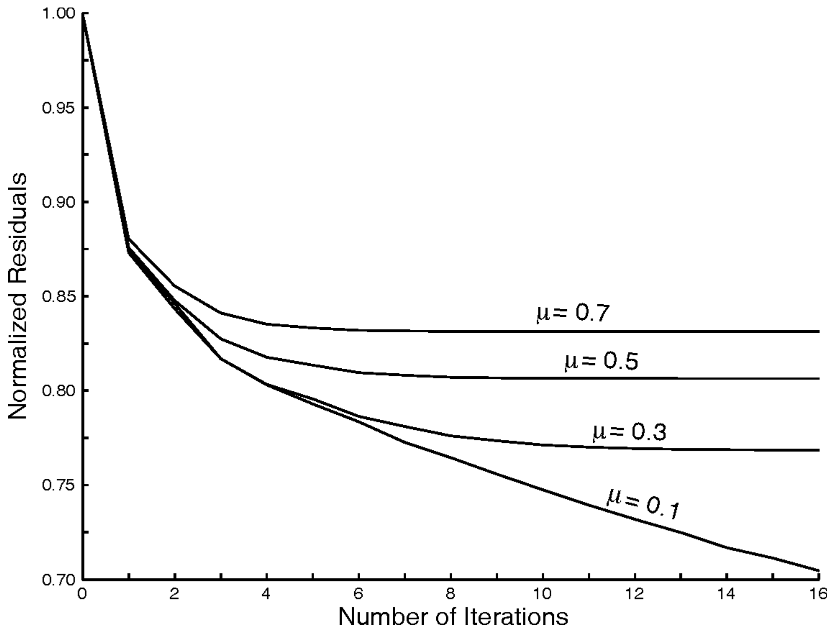

Figure 4. Convergence rates with different μ values.

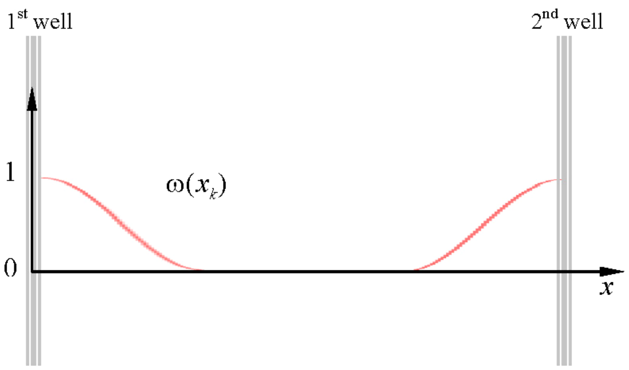

Figure 5. The diagrammatic curve of the relation between the weighting coefficient ω_k and the horizontal distance x_k of a particular cell.

coefficient. We set the weight ω_k here as an estimated certainty of the kth measurement, as

$$\omega_k = \begin{cases} 0.5 + 0.5\cos\left(\dfrac{x_a - x_k}{x_a}\pi\right), & \text{for} \quad x_k < x_a, \\ 0, & \text{for} \quad x_a < x_k < x_b, \\ 0.5 + 0.5\cos\left(\dfrac{x_k - x_b}{X - x_b}\pi\right), & \text{for} \quad x_k > x_b, \end{cases} \tag{13}$$

where x_k is the centre point position of kth cell in the x direction, X is the distance between the two wells. In this experiment, $X = 300$ m. We set $x_a = 50$ m, and $x_b = 250$ m, which means we use the logging information as a constraint at a 50 m range in the vicinity of each of two boreholes. Figure 5 shows the diagrammatic curve of the relation between ω_k and x_k : $\omega_k = 1$ at the well track and $\omega_k \to 0$ away from the wells.

Figure 6(a) is the initial velocity built with well-log constraints. As the initial velocity model is the mixture of the logging information and the time back-projection model, in the inversion, we set $\mathbf{C}_\mathrm{M}^{-1}$ as an identity matrix. Using the same the data certainty matrix $\mathbf{C}_\mathrm{D}^{-1}$ and the same parameter μ as in the previous experiment to solve equation (6), we obtain the well-log constrained velocity image as shown in figure 6(b).

The second scheme is to define the initial model purely from the logging information. As shown in figure 7(a), the velocity field between two wells is given by a simple linear interpolation between the two sonic logging curves, although a more sophisticated 2D interpolator could have been used. In the inversion, we defined the model covariance matrix as a diagonal weight matrix

$$\mathbf{C}_\mathrm{M}^{-1} = \kappa[\mathrm{diag}\{\omega_k\}], \tag{14}$$

where κ is estimated from the previous experiment (equation (11)). The arguments given for such weighting coefficients are that the inversion solution should have least deviation from the 'hard' geological evidence, such as the sonic logging information. The remaining part of the survey region may have more deviation, since the true velocity model might differ much more from the initial velocity estimate, as it is far away from the actual measurement (well logging), and the true ray paths might deviate much more from the initial ray paths.

Using the same data certainty matrix $\mathbf{C}_\mathrm{D}^{-1}$ and the same parameter μ as in the previous experiment, we obtained the well-log constrained velocity image as shown in figure 7(b), in which the distinct layered structure with high/low velocities corresponds to the high and low velocity intervals in the well logs.

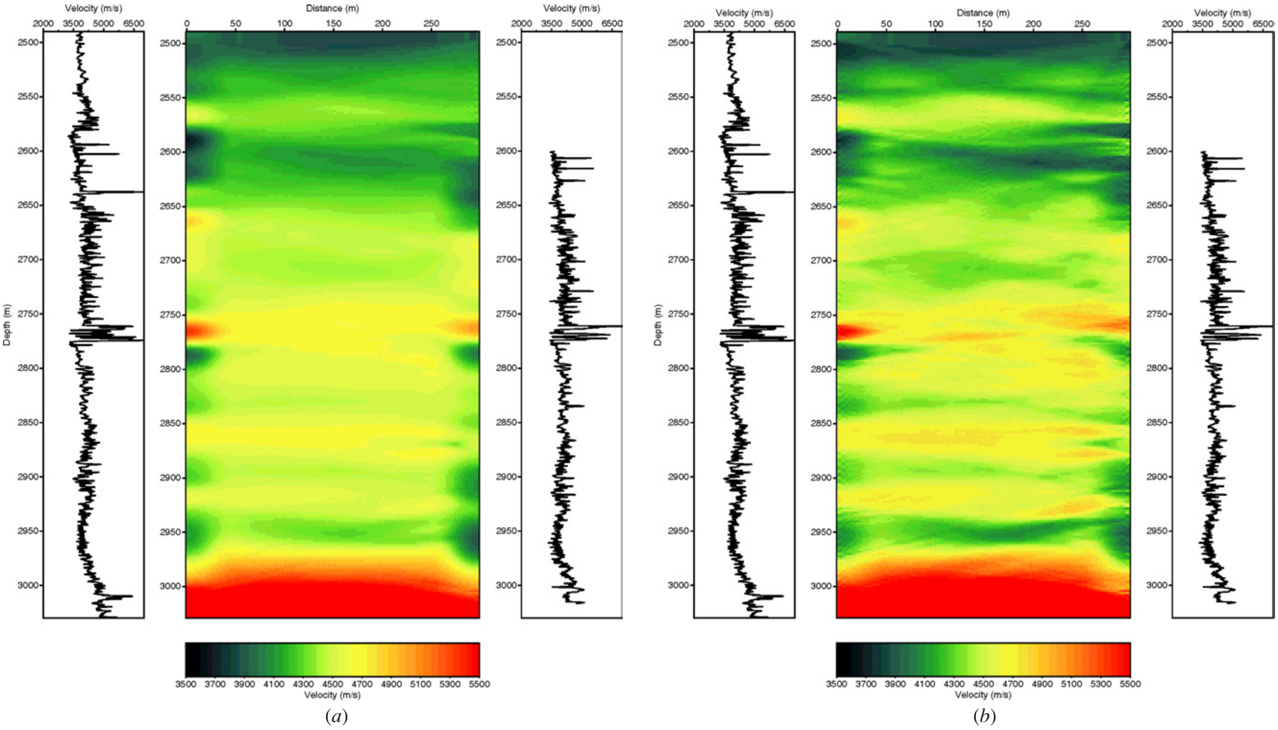

Figure 6. Well-log constraint scheme 1. (*a*) The initial velocity model is the weighted average of logging information from the two boreholes and the preliminary time back-projection tomogram. (*b*) The final tomographic image.

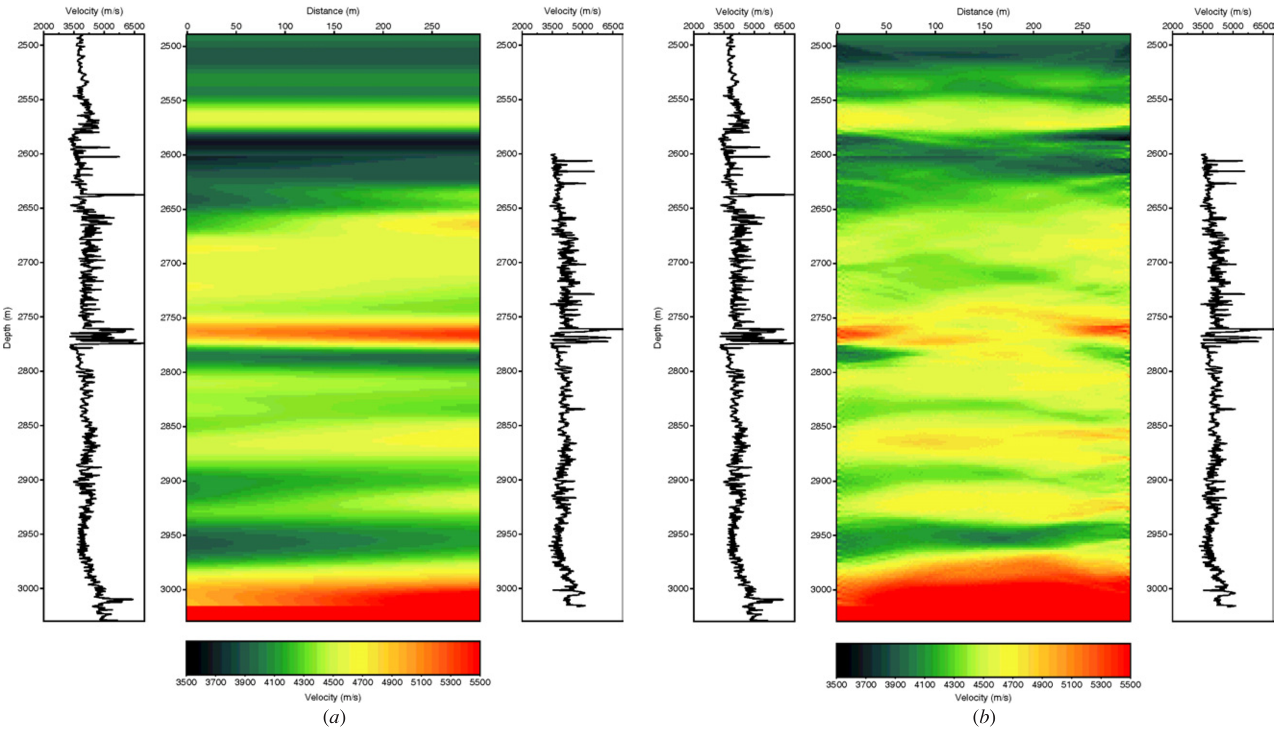

Figure 7. Well-log constraint scheme 2. (*a*) The initial model is simply a linear interpolation between the sonic logging curves from the two boreholes. (*b*) The final tomographic image using the initial model of figure (*a*) and a model covariance matrix defined as in figure 5.

Generally speaking, figures 6(*b*) and 7(*b*) are quite similar in terms of spatial velocity variation. But we prefer to use the first scheme, as its initial model uses both logging information and the preliminary imaging of travel time inversion.

6. Conclusions

Depending on how the experiment is conducted, the data may be inaccurate, insufficient and inconsistent, and may contain noise. Simple data fitting in an inversion is therefore generally inadequate. Modifying an improperly posed problem until it is properly posed and thereby solvable generally involves identifying a unique solution and stabilizing it with respect to perturbations of the data. In this paper, to address issues in real data crosshole seismic tomography, we have adopted a step-by-step strategy, which we believe is both practical and sensible:

(1) *The effect of data errors*. We manage to suppress the effect of the first arrival picking errors by providing a working definition to the conventional data covariance matrix, which is defined here as a data confidence matrix in terms of the vertical offset explicitly.
(2) *The balance between the data contribution and the a priori model*. We control it explicitly by the trade-off parameter μ in the inversion. To make the choice of μ meaningful and normalized, we use the normalizing factor κ systematically in advance.
(3) *Logging constraint*. After we have solved the above two issues, we start to bring in the well log information as a geological constraint in the inversion.

We perform the crosshole travel time inversion here as a linear inverse problem that solves for the slowness update, rather than the slowness field directly as in the classic crosshole travel time inversion. By carefully addressing these issues step by step, we would expect that the final tomographic image is not biased by any strong constraints.

Acknowledgments

Thanks to Professor S A Greenhalgh and two anonymous referees for a constructive review, and to H Cao, G J Chen and Y S Wu for helpful discussion. The crosshole seismic dataset is provided courtesy of the Nanjing Institute of Geophysical Prospecting, China.

References

Berryman J G 1989 Weighted least-squares criteria for seismic travel time tomography *IEEE Trans. Geosci. Remote Sens.* **27** 302–9
Bording R P, Gersztenkorn A, Lines L R, Scales J A and Treitel S 1987 Applications of seismic travel time tomography *Geophys. J. R. Astron. Soc.* **90** 285–303
Cao S and Greenhalgh S A 1995 Relative error based non-linear inversion: application to seismic travel time tomography *Geophys. J. Int.* **121** 684–94
Engl H W, Hanke M and Neubauer A 1996 *Regularization of Inverse Problems* (Dordrecht: Kluwer)
Groetsch C W 1993 *Inverse Problems in the Mathematical Sciences* (Braunschweig: Vieweg)
Hanke M 1995 *Conjugate Gradient Type Methods for Ill-Posed Problems* (Essex: Longman Scientific and Technical)
Rawlinson N and Sambridge M 2003 Irregular interface parametrization in 3-D wide-angle seismic travel time tomography *Geophys. J. Int.* **155** 79–92
Röhm A H E, Bijwaard H, Spakman W and Trampert J 2000 Effects of arrival time errors on travel time tomography *Geophys. J. Int.* **142** 270–6
Scales J A, Gersztenkorn A and Treitel S 1988 Fast ℓ_p solution of large, sparse, linear systems: application to seismic travel time tomography *J. Comput. Phys.* **75** 314–33
Spakman W and Bijwaard H 2001 Optimization of cell parametrizations for tomographic inverse problem *Pure Appl. Geophys.* **158** 1401–23
Tarantola A 2005 *Inverse Problem Theory and Methods for Model Parameter Estimation* (Philadelphia: SIAM)
van Wijk K, Scales J A, Navidi W and Tenorio L 2002 Data and model uncertainty estimation for linear inversion *Geophys. J. Int.* **149** 625–32
Wang Y 2003 *Seismic Amplitude Inversion in Reflection Tomography* (Oxford: Pergamon)
Wang Y and Houseman G A 1995 Tomographic inversion of reflection seismic amplitude data for velocity variation *Geophys. J. Int.* **123** 355–72
Wang Y and Pratt R G 1997 Sensitivities of seismic travel times and amplitudes in reflection tomography *Geophys. J. Int.* **131** 618–42
Wang Y, White R E and Pratt R G 2000 Seismic amplitude inversion for interface geometry: practical approach for application *Geophys. J. Int.* **142** 162–72
Worthington M H 1984 An introduction to geophysical tomography *First Break* **2** 20–6
Zhou B and Greenhalgh S A 2003 Crosshole seismic inversion with normalized full-waveform amplitude data *Geophysics* **68** 1320–30